Self-modulation of nonlinear Alfvén waves in a strongly magnetized relativistic electron-positron plasma

Rodrigo A. López,[1] Felipe A. Asenjo,[2] Víctor Muñoz,[1] Abraham C.-L. Chian,[3,4] and J. A. Valdivia[1,5,6]

[1]*Departamento de Física, Facultad de Ciencias, Universidad de Chile, Santiago, Chile*

[2]*Institute for Fusion Studies, The University of Texas at Austin, Austin, Texas, USA*

[3]*Observatoire de Paris, CNRS, Meudon, France*

[4]*National Institute for Space Research (INPE) and World Institute for Space Environment Research (WISER), São José dos Campos-SP, Brazil*

[5]*Centro para el Desarrollo de la Nanociencia y la Nanotecnología, CEDENNA, Santiago, Chile*

[6]*Centro de Estudios Interdisciplinarios Básicos y Aplicados en Complejidad, CEIBA complejidad, Bogotá, Colombia*

(Received 19 April 2013; published 19 August 2013)

We study the self-modulation of a circularly polarized Alfvén wave in a strongly magnetized relativistic electron-positron plasma with finite temperature. This nonlinear wave corresponds to an exact solution of the equations, with a dispersion relation that has two branches. For a large magnetic field, the Alfvén branch has two different zones, which we call the normal dispersion zone (where $d\omega/dk > 0$) and the anomalous dispersion zone (where $d\omega/dk < 0$). A nonlinear Schrödinger equation is derived in the normal dispersion zone of the Alfvén wave, where the wave envelope can evolve as a periodic wave train or as a solitary wave, depending on the initial condition. The maximum growth rate of the modulational instability decreases as the temperature is increased. We also study the Alfvén wave propagation in the anomalous dispersion zone, where a nonlinear wave equation is obtained. However, in this zone the wave envelope can evolve only as a periodic wave train.

DOI: 10.1103/PhysRevE.88.023105   PACS number(s): 52.27.Ep, 52.27.Ny, 52.35.Mw, 52.35.Sb

I. INTRODUCTION

Relativistic electron-positron plasmas have received much attention because they are relevant in several environments, of either an astrophysical or laboratory nature. Examples of this include accretion disks [1–3], models of the early universe [4,5], pulsar magnetospheres [6,7], hypothetical quark stars [8], ultraintense lasers [9], and laboratory and tokamak plasmas [10,11].

For example, in the magnetosphere of pulsars, particularly in millisecond pulsars, there must be strong electric fields that can accelerate charged particles along the magnetic field. In these environments, the particle number density can be estimated as $n_e \sim 10^{-1}(B/P)$ [12], where B is the magnetic field and P the period of the pulsar in cgs units. For $B \sim 10^{12}$ G and $P \sim 10^{-1}$ s we have $n_e \sim 10^{12}$ cm^{-3}. Under a dynamical situation, these values can increase by an order of magnitude [13]. When the magnetic field reaches a value $B > 4 \times 10^{13}$ G, for example, in magnetars, we can have other important effects in the production of electron-positron pairs such as photon splitting in a strong magnetic field [7] or electron-positron pair annihilation into a photon in the presence of a strong magnetic field [14]. Hence, large values of the electron positron density can be produced in these environments. For example, Da Costa *et al.* [15] used a value of $n_e = 10^{17}$ cm^{-3}, while Matsukiyo and Hada [16] used $\Omega/\omega_{pe} \approx 1$ with $\Omega = eB/mc$ and $\omega_{pe} = \sqrt{4\pi n_e e^2/m}$.

Several effects in these plasmas are related to wave propagation, such as the proposed pulsar radio emission processes [17], bulk acceleration of relativistic jets [18], and quasar relativistic jets [19], among others. We also know that in the presence of a strong magnetic field, Alfvén waves should play a fundamental role in plasmas, e.g., they are the ubiquitous by-product of magnetic reconnection in space, astrophysical and laboratory plasmas as evidenced by *in situ* spacecraft observations in the solar wind [20–22]. Recently, there is a growing interest in the study of magnetic reconnection in relativistic electron-positron plasmas [23–27] as well as nonlinear Alfvén waves in relativistic electron-positron plasmas, motivated by potential applications in astrophysics and laboratory experiments [19,28–31].

A number of papers have investigated the nonlinear propagation of Alfvén waves in relativistic electron-positron plasmas, in particular, the envelope soliton propagation, because it has been proposed as a mechanism for the production of micropulses in pulsars [32,33]. The model of Chian and Kennel in Ref. [32], which considers the self-modulation of a circularly polarized wave in a cold unmagnetized electron-positron plasma, has been improved by several authors [34–36]. In the same spirit, we use this model as a starting point for the case of magnetized plasmas.

The aim of this work is to study the self-modulation of a nonlinear Alfvén wave propagating along the ambient magnetic field in a strongly magnetized electron-positron plasma with fully relativistic temperatures, based on the theory of hot relativistic fluid formulated recently by Mahajan [37] in a covariant form, where the plasma and the electromagnetic fields are unified into a single field. In Ref. [38] the nonlinear dispersion relation for a circularly polarized electromagnetic wave in a hot pair plasma was derived by applying this formalism. The dispersion relation presents two branches in general: the electromagnetic and the Alfvén. Some features of both branches were studied in detail in Ref. [38]. Based on this formalism, the parametric decays [39] of these circularly polarized electromagnetic waves were studied. For the case of a weakly magnetized hot pair plasma in the electromagnetic branch the self-modulation of these waves was also analyzed and a nonlinear wave equation was derived, which produces a propagating wave train or a soliton [40]. In Ref. [38] it was shown that in addition to the typical Alfvén branch, the low-frequency branch has an anomalous dispersion zone, where $d\omega/dk$ is negative. Hence, it is the aim of this work to study the nonlinear nature of the Alfvén branch, for the normal and anomalous parts, in a relativistic electron-positron plasma.

This paper is organized as follows. In Sec. II the relativistic two fluid model with relativistic temperatures is presented and the dispersion relation for the circularly polarized wave solution is briefly derived. In Sec. III the approximations for the fluid velocity in the strongly magnetized case are discussed. In Sec. IV a nonlinear Schrödinger equation for the complex wave amplitude is derived in the normal dispersion zone of the Alfvén branch. In Sec. V we investigate the nonlinear behavior in the anomalous dispersion zone of the Alfvén branch. Finally, in Sec. VI, our results are summarized.

II. EXACT CIRCULARLY POLARIZED ELECTROMAGNETIC WAVE

In Ref. [37] a relativistic formalism is presented for a plasma where the electromagnetic field is coupled with the charged fluid through the enthalpy density that carries the statistical information of the system. The plasma dynamics is given by Maxwell's equations, the momentum equation for the relativistic fluid [37,38],

$$\left(\frac{\partial}{\partial t}+\vec{v}_j\cdot\vec{\nabla}\right)(f_j\gamma_j\vec{v}_j)=\frac{q_j}{m}\left(\vec{E}+\frac{1}{c}\vec{v}_j\times\vec{B}\right)-\frac{1}{mn_j}\vec{\nabla}p_j, \tag{1}$$

the pressure equation,

$$\gamma_j\left(\frac{\partial}{\partial t}+\vec{v}_j\cdot\vec{\nabla}\right)p_j=mn_jc^2\left(\frac{\partial}{\partial t}+\vec{v}_j\cdot\vec{\nabla}\right)f_j, \tag{2}$$

and the continuity equation,

$$\frac{\partial n_j}{\partial t}+\vec{\nabla}\cdot(n_j\,\vec{v}_j)=0, \tag{3}$$

where j is the species index ($j=p$ for positrons and $j=e$ for electrons), m is the electron mass, $\vec{v}_j$ is the velocity of each fluid, c is the speed of light, γ_j is the relativistic Lorentz factor, n_j is the density in the laboratory frame, p_j is the pressure, $q_j=-\eta_j e$ is the charge (with $\eta_e=1$ and $\eta_p=-1$), and f_j is a relativistic thermal factor. The f_j factor is related to the enthalpy density $h_j=mc^2n_jf_j/\gamma_j$ and depends only on the thermodynamical properties of the plasma. Starting from the canonical partition function, and assuming a Maxwell-Jüttner equilibrium distribution for the relativistic particles [37,38,41], we can derive $f_j=f(\mu_j)=K_3(\mu_j)/K_2(\mu_j)$, where K_2 and K_3 are the modified Bessel functions of order 2 and 3, respectively, and $\mu_j=mc^2/k_BT_j$, where T_j is the temperature, and k_B is the Boltzmann constant. In the cold plasma limit we have $f_j=1$, so Eq. (1) becomes the relativistic momentum equation for a cold plasma. On the other hand, in the high-temperature limit, $f_j\approx 4/\mu_j$. Hence, the relativistic effects of the particle motion in the wave field are included in a consistent way through the relativistic factor γ and in the thermal motion by means of the function f. In order to close the system of Eqs. (1), (2), and (3) we consider the equation of state $p_j=n_jk_BT_j/\gamma_j$ for an ideal gas, which is consistent with the above particle distribution. In the Lorentz gauge, the wave equation for the vector potential is

$$\frac{\partial^2\vec{A}}{\partial t^2}-c^2\nabla^2\vec{A}=4\pi nec(\vec{v}_p-\vec{v}_e), \tag{4}$$

where electrons and positrons have equal constant densities, $n_e=n_p=n$.

As shown in Ref. [38], we can find an exact nonlinear transverse solution for the relativistic fluid equations. The circularly polarized electromagnetic wave, in terms of the vector potential, can be written as

$$\vec{A}=a_0[\cos(kz-\omega t)\hat{x}+\sin(kz-\omega t)\hat{y}]. \tag{5}$$

This wave of arbitrary amplitude can propagate in a relativistic electron-positron plasma along a constant background magnetic field $B_0\hat{z}$ and induces a purely transverse velocity for each fluid, given by

$$\vec{v}_j=\eta_j\frac{e\vec{A}}{mc}\left(\frac{\omega}{f_j\gamma_j\omega+\eta_j\Omega_c}\right), \tag{6}$$

where $\Omega_c=eB_0/(mc)$ is the positron gyrofrequency and the relativistic Lorentz factor is

$$\gamma_j=\left(1-\frac{|\vec{v}_j{}^2|}{c^2}\right)^{-1/2}. \tag{7}$$

From Eqs. (4) and (6) it is straightforward to obtain the dispersion relation,

$$\omega^2-c^2k^2=\omega_{pe}^2\left(\frac{\omega}{f_e\gamma_e\omega+\Omega_c}+\frac{\omega}{f_p\gamma_p\omega-\Omega_c}\right), \tag{8}$$

where $\omega_{pe}^2=4\pi ne^2/m$ is the electron plasma frequency. Notice that the plasma frequency is defined in the laboratory frame. We can also write this dispersion relation as a function of the velocity of the fluids [38],

$$\omega^2-c^2k^2=-\frac{\omega_{pe}^2}{c\sqrt{\lambda}A}(v_p-v_e), \tag{9}$$

where $\lambda=e^2/(m^2c^4)$ and $A=|\vec{A}|$ is the module of the vector potential. It will become convenient to use the normalized variables $x=\omega/\Omega_c$, $y=ck/\Omega_c$, and $\alpha=\omega_{pe}/\Omega_c$. Notice that the dispersion relation must be solved simultaneously with Eqs. (6) and (7), which can be done numerically. This wave represents a uniform nonlinear solution that satisfies the dispersion relation and that can propagate in the electromagnetic and Alfvén branches [38].

We note that, in general, the fluid velocity depends on $\vec{A}$ [see Eq. (6)], giving rise to a nonlinear wave equation for $\vec{A}$. It was proven in Ref. [40] that in the weakly magnetized regime, this dependence of the velocity on $\vec{A}$ leads to the appearance of solitons for waves that propagate in the plasma. The nonlinearity is introduced through the velocities and the relativistic factors γ and corresponds to the electromagnetic branch of the dispersion relation.

For the case of low-frequency Alfvén waves in a strongly magnetized plasma, an analytical treatment can be done. This is the regime where the nonlinear effects of Alfvén modes will be studied, as described in the following section, where we obtain the nonlinear Schrödinger equation for the Alfvén wave propagation.

III. THE STRONGLY MAGNETIZED PLASMA

The low-frequency modes can be studied in the strongly magnetized limit for relativistic electron-positron plasmas. This low-frequency regime corresponds to the Alfvén branch of the dispersion relation (8) (see below). In the strongly magnetized limit $x \ll 1$ we can use approximate expressions for the velocities to capture the main nonlinear effects produced by the vector potential in the relativistic factors. First, we can assume that the direction of the velocity is given by the vector potential, such that

$$\vec{v}_j = v_j \frac{\vec{A}}{A}. \tag{10}$$

It follows that Eq. (6) can be rewritten as

$$\frac{v_j}{c} = \eta_j \sqrt{\lambda} A \left(\frac{x}{f \gamma_j x + \eta_j} \right), \tag{11}$$

where we assume equal temperatures for each species $\mu_e = \mu_p = \mu$, so $f_e = f_p = f$. Replacing the relativistic factor (7) in Eq. (11), we obtain the following equation for the velocity of each fluid,

$$v_j^4 - c^2 v_j^2 - \left(f_j^2 + \lambda A^2\right) c^2 x^2 v_j^2 - 2\eta_j x f_j c^2 v_j^2 \left(1 - \frac{v_j^2}{c^2}\right)^{1/2} + \lambda A^2 c^4 x^2 = 0. \tag{12}$$

This exact equation can be solved analytically in the strongly magnetized limit $x \ll 1$ to get approximate expansions for the velocities, which are

$$\frac{v_{j1}}{c} = -\eta_j + \eta_j \frac{f^2 x^2}{2} + \eta_j \frac{f^4 x^4}{8} - \sqrt{\lambda} A f^2 x^3 + \frac{3}{2} \eta_j \lambda A^2 f^2 x^4 - \sqrt{\lambda} A f^2 (f^2 + 2\lambda A^2) x^5, \tag{13}$$

$$\frac{v_{j2}}{c} = \sqrt{\lambda} A (x - \eta_j f x^2 + f^2 x^3) - \frac{\eta_j}{2} \sqrt{\lambda} A f (2f^2 + \lambda A^2) x^4 + \sqrt{\lambda} A f^2 (f^2 + 2\lambda A^2) x^5, \tag{14}$$

$$\frac{v_{j3}}{c} = \sqrt{\lambda} A (x + \eta_j f x^2 + f^2 x^3) + \frac{\eta_j}{2} \sqrt{\lambda} A f (2f^2 + \lambda A^2) x^4 + \sqrt{\lambda} A f^2 (f^2 + 2\lambda A^2) x^5, \tag{15}$$

$$\frac{v_{j4}}{c} = \eta_j - \eta_j \frac{f^2 x^2}{2} - \eta_j \frac{f^4 x^4}{8} - \sqrt{\lambda} A f^2 x^3 - \frac{3}{2} \eta_j \lambda A^2 f^2 x^4 - \sqrt{\lambda} A f^2 (f^2 + 2\lambda A^2) x^5. \tag{16}$$

In order to study the dominant nonlinear effects in the wave equation [Eq. (4)], we have considered the expansion for the velocities up to order $\mathcal{O}(x^5)$, otherwise the wave equation will be linear in $\vec{A}$ and no interesting effects will appear (see below).

Each solution turns out to correspond to a different zone of the Alfvén branch. In order to identify which solution is associated to which zone, Fig. 1 shows the exact numerical solution for the velocity (11) (dotted black line) for both positrons and electrons.

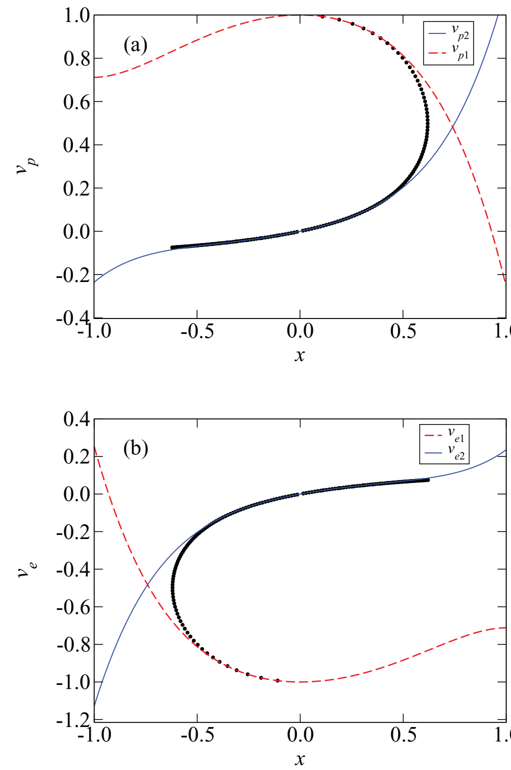

FIG. 1. (Color online) Velocity vs normalized frequency $x = \omega/\Omega_c$ for $\sqrt{\lambda} A = 0.2$, $1/\mu = 0.02$, and $\omega_{pe}/\Omega_c = 1$. Dotted (black) line: exact solution [Eq. (11)]. (a) Positron velocity. The solid (blue) line is the approximate solution v_{p2} [Eq. (14)]; the dashed (red) line is the approximate solution v_{p1} [Eq. (13)]. (b) Electron velocity. The solid (blue) line is the approximate solution v_{e2} [Eq. (14)]; the dashed (red) line is the approximate solution v_{e1} [Eq. (13)].

Let us now consider only the exact solutions for positrons, Fig. 1(a). For $x > 0$, there are two possible solutions. One of these solutions tends to zero when $x \to 0$, and the other one tends to one for $x \to 0$. When comparing with Fig. 1 in Ref. [38], it follows that the first one corresponds to the normal dispersion zone and the other one to an anomalous dispersion zone, where $d\omega/dk$ is negative. In this anomalous zone the positrons resonate with the Alfvén wave, so the velocity tends to the speed of light. The same occurs to the electrons but for $x < 0$, as seen in Fig. 1(b): producing another anomalous zone, where $v_e/c \to -1$ for $x \to 0$.

We have also plotted the approximate solutions in Eqs. (13)–(16) for both positrons and electrons. Figure 1 shows that, for positrons, the two relevant solutions near $x \ll 1$ are v_{p1} and v_{p2}; for electrons, they are v_{e1} and v_{e2}. In Fig. 1(a) the solid (blue) line corresponds to v_{p2} [Eq. (14)] and approximates the exact solution in the normal dispersion zone. The dashed (red) line is v_{p1} [Eq. (13)], which describes the anomalous dispersion zone. Note the good agreement with the exact solution when $x \ll 1$ for both cases. For the electrons, Fig. 1(b), the solid (blue) line is v_{e2} [Eq. (14)], which lies in the normal dispersion zone, whereas the dashed (red) line is v_{e1} [Eq. (13)], which describes the anomalous dispersion zone. Again, note the agreement when $x \ll 1$ for both situations.

IV. NORMAL DISPERSION ZONE OF THE ALFVÉN BRANCH

A. Nonlinear Schrödinger equation for wave amplitude

We now study the behavior of a circularly polarized wave in the normal Alfvén dispersion zone in the limit $|x| \ll 1$. As shown in Sec. III (see Fig. 1), for this zone the approximate solutions for the velocities are given by Eq. (14) for electrons and positrons,

$$\frac{v_e}{c} = \sqrt{\lambda}A(x - fx^2 + f^2x^3) - \frac{1}{2}\sqrt{\lambda}Af(2f^2 + \lambda A^2)x^4 + \sqrt{\lambda}Af^2(f^2 + 2\lambda A^2)x^5, \tag{17}$$

$$\frac{v_p}{c} = \sqrt{\lambda}A(x + fx^2 + f^2x^3) + \frac{1}{2}\sqrt{\lambda}Af(2f^2 + \lambda A^2)x^4 + \sqrt{\lambda}Af^2(f^2 + 2\lambda A^2)x^5. \tag{18}$$

We replace these approximations in the dispersion relation Eq. (9), and we obtain the approximate dispersion relation, in the same limit, as

$$x^2 - y^2 + \alpha^2 fx^2[2 + x^2(2f^2 + \lambda A^2)] = 0. \tag{19}$$

We can see in Fig. 2 that this approximate dispersion relation perfectly describes the normal Alfvén dispersion zone, in the relevant limit, $|x| \ll 1$. With these approximate solutions for the velocities, the wave equation for the vector potential Eq. (4) becomes

$$\frac{\partial^2 \vec{A}}{\partial t^2} - c^2\frac{\partial^2 \vec{A}}{\partial z^2} - \omega_{pe}^2 fx^2[2 + x^2(2f^2 + \lambda A^2)]\vec{A} = 0. \tag{20}$$

In order to study the modulational instability, we introduce a space-dependent complex modulational representation for the amplitude of the circularly polarized electromagnetic wave,

$$\vec{A} = \tfrac{1}{2}[a(z,t)e^{-i\omega t}\,\hat{h} + a(z,t)^* e^{i\omega t}\,\hat{h}^*], \tag{21}$$

where

$$\hat{h} = \frac{\hat{x} - i\hat{y}}{\sqrt{2}}.$$

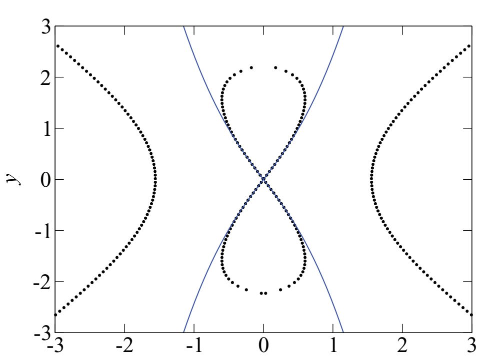

FIG. 2. (Color online) Dispersion relation, normalized wave number $y = ck/\Omega_c$ vs normalized frequency $x = \omega/\Omega_c$ for $\sqrt{\lambda}A = 0.2$, $1/\mu = 0.04$, and $\alpha = 1$. The dotted (black) line is the exact numerical solution of the dispersion relation (8). The solid (blue) line represents the solution of the approximated dispersion relation (19) valid for $|x| \ll 1$.

If no modulation occurs,

$$a(z,t) = \sqrt{2}\,a_0 e^{ikz}. \tag{22}$$

Then, taking a slowly time-varying modulation, so $\partial_t^2 a \ll \omega^2 a$, Eq. (20) yields an equation for $a(z,t)$,

$$i\frac{\partial a}{\partial t} + \frac{c^2}{2\omega}\frac{\partial^2 a}{\partial z^2} + \left\{\frac{\omega}{2} + \alpha^2 f\omega\left[1 + \frac{\omega^2}{4\Omega_c^2}(4f^2 + \lambda|a|^2)\right]\right\}a = 0. \tag{23}$$

Defining

$$P(\omega) = \frac{c^2}{2\omega}, \tag{24}$$

$$R(\omega,|a_0|^2) = \frac{\omega}{2} + \alpha^2 f\omega\left(1 + \frac{\omega^2 f^2}{\Omega_c^2}\right) + Q(\omega)|a_0|^2, \tag{25}$$

$$Q(\omega) = \frac{\alpha^2}{4\Omega^2} f\lambda\omega^3, \tag{26}$$

we can rewrite the wave equation [Eq. (23)] as

$$i\frac{\partial a}{\partial t} + P(\omega)\frac{\partial^2 a}{\partial z^2} + R(\omega,|a_0|^2)a + Q(\omega)(|a|^2 - |a_0|^2)a = 0. \tag{27}$$

Note that in Eq. (27) we have added and subtracted a term proportional to $|a_0|^2$. Thus, we make sure that when Eq. (22) holds, then Eq. (27) becomes Eq. (19), that is, the dispersion relation for the unperturbed electromagnetic wave in the strongly magnetized limit.

Finally, Eq. (27) can be written as a nonlinear Schrödinger equation by changing $a \longrightarrow a\exp(iR(\omega,|a_0|^2)t)$, namely

$$i\frac{\partial a}{\partial t} + P(\omega)\frac{\partial^2 a}{\partial z^2} + Q(\omega)(|a|^2 - |a_0|^2)\,a = 0. \tag{28}$$

B. Modulational instability

From Eqs. (24) and (26), it follows that $P(\omega)$ and $Q(\omega)$ have the same sign, and, therefore, the necessary condition for a modulational instability [42] is fulfilled. To study the stability of the modulation, we decompose a as [32]

$$a = \sqrt{\rho(z,t)}\exp[i\sigma(z,t)], \tag{29}$$

so Eq. (28) becomes

$$\begin{aligned} 0 &= \frac{\partial \rho}{\partial t} + 2P\frac{\partial}{\partial z}\left(\rho\frac{\partial \sigma}{\partial z}\right), \\ Q(\rho - \rho_0) &= \frac{\partial \sigma}{\partial t} + P\left[\frac{1}{4\rho^2}\left(\frac{\partial \rho}{\partial z}\right)^2 - \frac{1}{2\rho}\frac{\partial^2 \rho}{\partial z^2} + \left(\frac{\partial \sigma}{\partial z}\right)^2\right], \end{aligned} \tag{30}$$

where $\rho_0 = |a_0|^2$. Linearizing these equations

$$\rho = \rho_0 + \rho_1 e^{ik_L z - \omega_L t}, \quad \sigma = \sigma_1 e^{ik_L z - \omega_L t},$$

where ρ_1 and σ_1 are first-order quantities, we obtain the low-frequency modulation dispersion relation,

$$\omega_L^2 = P^2 k_L^4 - 2PQ\rho_0 k_L^2, \tag{31}$$

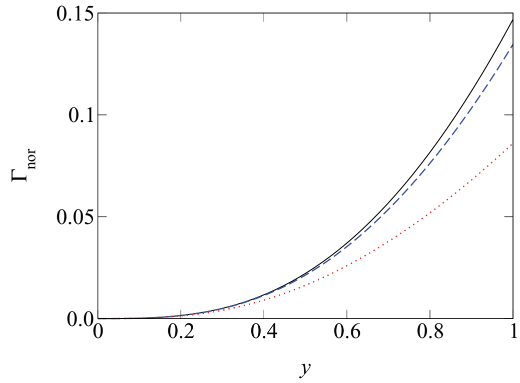

FIG. 3. (Color online) Normalized maximum growth rate, Eq. (32), as a function of $y = ck/\Omega_c$. We use $\omega_{pe}/\Omega_c = 1$ and $\sqrt{\lambda}A = 0.2$. Solid (black) line: $1/\mu = 0.01$. Dashed (blue) line: $1/\mu = 0.1$. Dotted (red) line: $1/\mu = 0.5$.

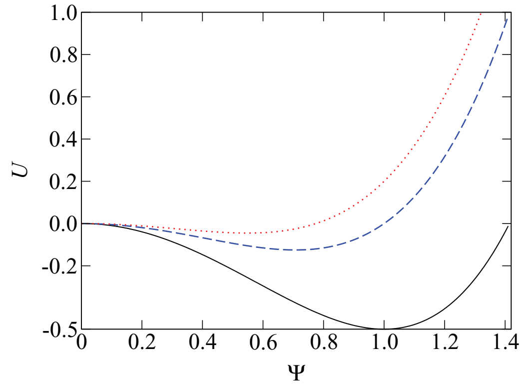

FIG. 4. (Color online) Sagdeev potential $U(\Psi)$, Eq. (36). Solid (black) line: $\tau = 0$. Dashed (blue) line: $\tau = 1$. Dotted (red) line: $\tau = 1.4$.

that has a maximum growth rate given by $\Gamma = Q\rho_0$. In Fig. 3 we plot the normalized maximum growth rate defined by

$$\Gamma_{\rm nor} = \frac{4\Gamma}{\lambda\omega_{pe}\rho_0} = \alpha f x^3, \tag{32}$$

as a function of the normalized wave number y obtained from the approximate dispersion relation [Eq. (19)]. As we increase the temperature the maximum growth rate becomes smaller. This is due to the fact that for $x \ll 1$ in the normal zone this dispersion relation becomes $x = y/\sqrt{1+2\alpha^2 f}$, and, as the temperature increases, ($f \gg 1$) the growth rate behaves as $\Gamma_{\rm nor} \approx y^3/(\alpha^2\sqrt{8f})$. Moreover, in contrast with the weakly magnetized case (electromagnetic branch) [40], here the growth rate increases with the wave number.

When the modulation grows, the instability evolves into a nonlinear state balancing the dispersion with the nonlinearity. To study these nonlinear states, we focus on Eq. (28) for $a(z,t)$ and define the normalized variable,

$$\frac{a(z,t)}{a_0} = \Psi(\xi)e^{i\eta}, \tag{33}$$

where $\xi = (Qa_0^2/2P)^{1/2}\chi$ and $\chi = z - Vt$. Here V is the effective group velocity of the wave packet [43] and

$$\eta = \frac{V}{2P}z - \left(\frac{V^2}{4P} + \frac{Qa_0^2}{2}\tau^2\right)t,$$

with τ a parameter to be varied. Using Eq. (33) in Eq. (28), we obtain

$$\frac{d^2\Psi}{d\xi^2} = (2-\tau^2)\Psi - 2\Psi^3. \tag{34}$$

From Ref. [40] we know that the solutions of this equation can vary from periodic wave trains to localized solitons for different values of τ (see Fig. 2 in Ref. [40]). We can see this clearly when Eq. (34) is cast in the form of an energy integral equation using the Sagdeev potential approach [44],

$$\frac{1}{2}\left(\frac{d\Psi}{d\xi}\right)^2 + U(\Psi) = 0, \tag{35}$$

where the potential is given by

$$U(\Psi) = \frac{\Psi^4}{2} - \frac{2-\tau^2}{2}\Psi^2, \tag{36}$$

with the boundary condition $U(0) = 0$. We use this potential to make an analogy with an oscillator in a potential well. The potential is positive for $\Psi > \sqrt{2-\tau^2}$ and negative between the nulls $\Psi = 0$ and $\Psi = \sqrt{2-\tau^2}$ (see Fig. 4). Hence, there is a soliton $0 < \Psi < \sqrt{2-\tau^2}$, if $0 < |\tau| < \sqrt{2}$.

As a particular case, we now consider $\tau = 1$ and $\Psi'(0) = 0$. In this case we have a localized solitary wave solution $\Psi = \mathrm{sech}(\xi)$ [40,45], so the solution of Eq. (34) is

$$a(z,t) = a_0\mathrm{sech}\left(\sqrt{\frac{Qa_0^2}{2P}}\,\chi\right)e^{i\eta} \tag{37}$$

and, therefore,

$$\rho(z,t) = |a(z,t)a^*(z,t)| = \rho_0\mathrm{sech}^2(\sqrt{f}x^2\bar{\xi}), \tag{38}$$

where $\bar{\xi} = \omega_{pe}/(2c)\sqrt{\lambda\rho_0}\,\chi$. This solution is an envelope soliton because the envelope of the wave packet has the form of a solitary wave. In Fig. 5 we plot this solution in terms of the temperature and the wave number. In Fig. 5(a) we plot ρ as a function of $\bar{\xi}$ and $1/\mu$. Note that the soliton tends to become wider as the temperature increases because the solution will have the form $\rho \approx \rho_0\mathrm{sech}^2(y^2\bar{\xi}/2\alpha^2\sqrt{f})$. In Fig. 5(b) we plot ρ as a function of $\bar{\xi}$ and y, as obtained from the dispersion relation [Eq. (19)]. Here the localization of the soliton increases with wave number y, in contrast with the weakly magnetized case [40].

V. ANOMALOUS DISPERSION ZONE OF THE ALFVÉN BRANCH

A. Dispersion relation

Now we investigate the anomalous dispersion zone present in the Alfvén branch. In Sec. III we obtained the approximate solution for the velocity (6), and we identified the corresponding solutions for the normal and anomalous dispersion zones. To get the first nonlinear corrections to the wave equation given in (4), we keep terms up to order $\mathcal{O}(x^2)$. Later in the section, we will see that if we consider terms up to order $\mathcal{O}(x^5)$, the final

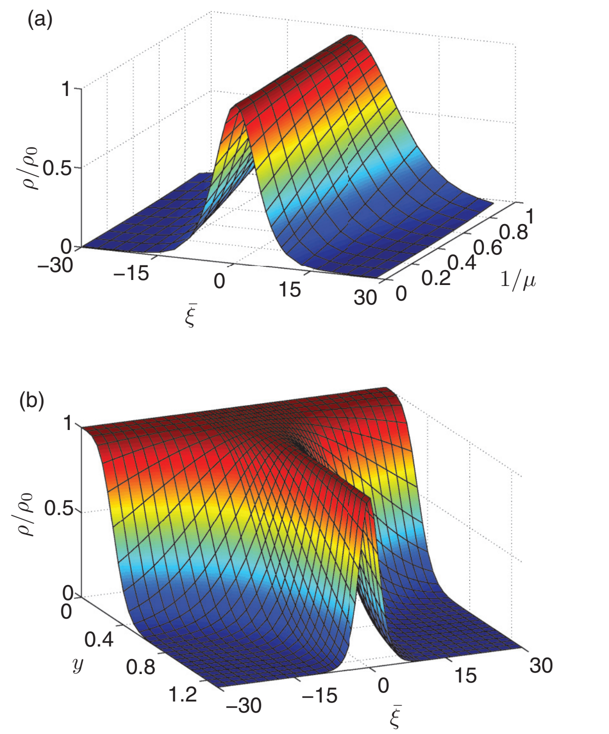

FIG. 5. (Color online) (a) Soliton solution [Eq. (38)] as a function of $\bar{\xi}$ and $1/\mu = k_B T/(mc^2)$ for $y = 0.8$. (b) Same solution but as a function of y for $1/\mu = 0.1$.

result will not change significantly. We focus our attention in the first quadrant of the dispersion relation $x,y \geqslant 0$. As shown in Sec. III and Fig. 1, the correct approximations for the velocities are Eq. (14) for electrons and Eq. (13) for positrons, hence,

$$\frac{v_e}{c} = \sqrt{\lambda}A(x - fx^2), \tag{39}$$

$$\frac{v_p}{c} = 1 - \frac{1}{2}f^2x^2. \tag{40}$$

Notice that, for $x,y \geqslant 0$, the positrons resonate with the circularly polarized Alfvén wave, so their velocity in the anomalous dispersion zone approaches the speed of light. On the other hand, the electrons do not resonate, so their velocity tends to zero in the anomalous zone. The dispersion relation (9) then becomes

$$x^2 - y^2 + \alpha^2\left[\frac{1}{\sqrt{\lambda}A}\left(1 - \frac{f^2x^2}{2}\right) - x(1 - fx)\right] = 0. \tag{41}$$

In Fig. 6 we compare this approximate dispersion relation with the exact one [Eq. (8)], showing a good similarity of both results in the anomalous zone.

B. Nonlinear Schrödinger equation for wave amplitude

Substituting Eqs. (39), (40), and Eq. (10) in the wave equation [Eq. (4)] yields

$$\frac{\partial^2 \vec{A}}{\partial t^2} - c^2\frac{\partial^2 \vec{A}}{\partial z^2} = \omega_{pe}^2\left[\left(1 - \frac{f^2x^2}{2}\right)\frac{1}{\sqrt{\lambda}A} - x(1 - fx)\right]\vec{A}. \tag{42}$$

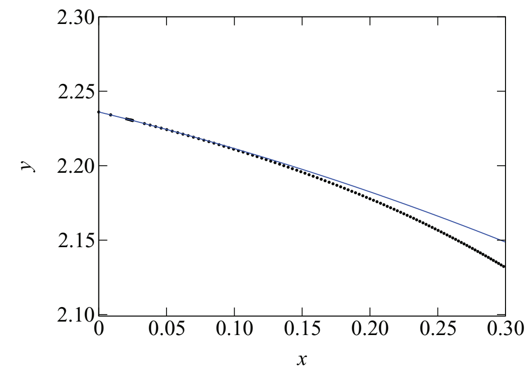

FIG. 6. (Color online) Dispersion relation in the anomalous zone, normalized frequency $x = \omega/\Omega_c$ versus normalized wave number $y = ck/\Omega_c$ for $\sqrt{\lambda}A = 0.2$, $1/\mu = 0.04$, and $\alpha = 1$. The dotted (black) line is the exact solution of the dispersion relation (8). The straight (blue) line is the approximate solution of dispersion relation (41).

As in the previous cases, we use the space-dependent complex modulational representation for the vector potential [Eq. (21)] and take the limit of a slowly time-varying modulation $\partial_t^2 a \ll \omega^2 a$. We obtain

$$i\frac{\partial a}{\partial t} + \frac{c^2}{2\omega}\frac{\partial^2 a}{\partial z^2} + \left[\frac{\omega}{2} - \frac{\omega_{pe}^2}{2\Omega_c}\left(1 - \frac{f\omega}{\Omega_c}\right)\right]a + \frac{1}{\sqrt{2\lambda}}\frac{\omega_{pe}^2}{\omega}\left(1 - \frac{f^2\omega^2}{2\Omega_c^2}\right)|a|^{-1}a = 0. \tag{43}$$

Let us note the $|a|^{-1}$ in the nonlinear factor. As before we define

$$P(\omega) = \frac{c^2}{2\omega}, \tag{44}$$

$$R(\omega) = \frac{\omega}{2} - \frac{\omega_{pe}^2}{2\Omega_c}\left(1 - \frac{f\omega}{\Omega_c}\right) + Q(\omega)|a_0|^{-1}, \tag{45}$$

$$Q(\omega) = \frac{\omega_{pe}^2}{\sqrt{2\lambda}\omega}\left(1 - \frac{f^2\omega^2}{2\Omega_c^2}\right), \tag{46}$$

so the wave equation becomes

$$i\frac{\partial a}{\partial t} + P(\omega)\frac{\partial^2 a}{\partial z^2} + R(\omega)a + Q(\omega)(|a|^{-1} - |a_0|^{-1})a = 0.$$

If no modulation occurs [see Eq. (22)], we recover the dispersion relation Eq. (41). Now, using the same transformation as in Sec. IV, $a \longrightarrow a\exp(iR(\omega,|a_0|^2)t)$, we obtain a nonlinear Schrödinger equation with a power-law nonlinearity,

$$i\frac{\partial a}{\partial t} + P(\omega)\frac{\partial^2 a}{\partial z^2} + Q(\omega)(|a|^{-1} - |a_0|^{-1})a = 0. \tag{47}$$

To study the nonlinear behavior in the anomalous zone, we define the variable

$$a(z,t) = a_0\Psi(\xi)e^{i\eta}, \tag{48}$$

where the new variable Ψ depends on $\xi = (Q/2Pa_0)^{1/2}\chi$, with $\chi = z - Vt$ and

$$\eta = \frac{V}{2P}z - \left(\frac{V^2}{4P} + \frac{Q}{2a_0}\tau^2\right)t.$$

Putting Eq. (48) in Eq. (47), we obtain the equation

$$\frac{\partial^2\Psi}{\partial\xi^2} = (2-\tau^2)\Psi - 2. \tag{49}$$

This is a linear equation that depends on the parameter τ and the initial conditions $\Psi(0)$ and $\Psi'(0)$. To have a better insight on the nature of the above equation, we can write it using the Sagdeev potential approach $(d\Psi/d\xi)^2/2 + U(\Psi) = 0$, with the potential

$$U(\Psi) = 2\Psi - \frac{2-\tau^2}{2}\Psi^2, \tag{50}$$

with $U(0) = 0$. We separate the study of this potential in three cases. First, for $\tau^2 < 2$, the potential is zero at $\Psi = 0$ and $\Psi = 4/(2-\tau^2) > 0$. From this we can see that in the range $0 < \Psi < 4/(2-\tau^2)$ the potential is positive, and for $\Psi > 4/(2-\tau^2)$ the potential is negative. Therefore, there is no confined structure for $U < 0$ and no soliton solution for this case. For $\tau^2 = 2$, the potential is always positive for $\Psi > 0$ and $U = 0$ only for $\Psi = 0$, so there is no soliton in this case either. Finally, for $\tau^2 > 2$, the potential is always positive for $\Psi > 0$. Hence, for all cases, there are no soliton solutions in the anomalous zone.

Let us examine the particular case $\tau^2 \neq 2$, with boundary conditions $\Psi(0) = 1$ and $\Psi'(0) = 0$. In this case, the solution of Eq. (49) is

$$\Psi(\xi) = \frac{1}{\tau^2-2}[\tau^2\cosh(\xi\sqrt{2-\tau^2}) - 2]. \tag{51}$$

For $\tau^2 < 2$, this solution diverges at $\xi \to \pm\infty$. So the only possible physical solution is periodic wave trains for $\tau^2 > 2$, namely

$$\Psi(\xi) = \frac{1}{\tau^2-2}[\tau^2\cos(\xi\sqrt{\tau^2-2}) - 2]. \tag{52}$$

As an illustration, Fig. 7 shows $\Psi(\xi)$ for $\tau^2 = 3$, in which case

$$\Psi(\xi) = 3\cos(\xi) - 2. \tag{53}$$

Using Eq. (48) we then can find

$$a(z,t) = \left[3\cos\left(\sqrt{\frac{Q}{2Pa_0}}\,\chi\right) - 2\right]e^{i\eta} \tag{54}$$

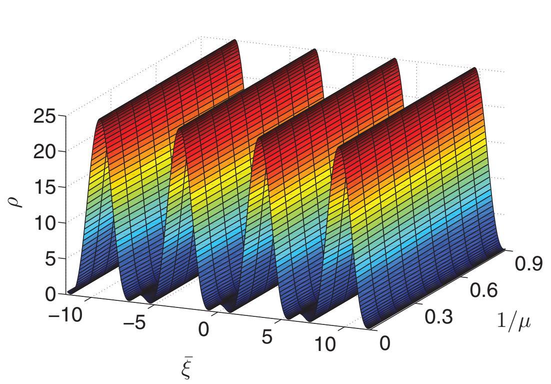

FIG. 7. (Color online) Solution Eq. (55) as function of $\bar{\xi}$ and $1/\mu = k_BT/(mc^2)$ for $y = 2.22$.

and, therefore,

$$\rho(z,t) = \left[3\cos\left(\sqrt{1-\frac{f^2x^2}{2}}\,\bar{\xi}\right) - 2\right]^2, \tag{55}$$

where $\bar{\xi} = (\omega_{pe}/c)(\sqrt{2\lambda}a_0)^{-1/2}\chi$. It becomes clear that the temperature and the wave number have a very little effect on the wave profile since x^2f^2 is small, as shown in Fig. 7, where we plot the periodic solution Eq. (55) in terms of the temperature.

One may wonder if an expansion to x^5 for the velocities (39) and (40), the same order considered in Sec. IV, could introduce a new nonlinear effect to produce a soliton behavior. Instead of Eq. (47), we would have an equation of the form

$$i\frac{\partial a}{\partial t} + P(\omega)\frac{\partial^2 a}{\partial z^2} + Q(\omega)|a|^{-1}a + S(\omega)|a|a + T(\omega)|a|^2 a = 0, \tag{56}$$

where

$$P(\omega) = \frac{c^2}{2\omega}, \tag{57}$$

$$Q(\omega) = \frac{\omega_{pe}^2}{\sqrt{2\lambda}\omega}\left(1 - \frac{f^2\omega^2}{2\Omega_c^2} - \frac{f^4\omega^4}{8\Omega_c^4}\right), \tag{58}$$

$$S(\omega) = -\frac{3\sqrt{2\lambda}}{8}\omega_{pe}^2 f^2\frac{\omega^3}{\Omega_c^4}, \tag{59}$$

$$T(\omega) = \frac{f\lambda}{8}\frac{\omega_{pe}^2\omega^3}{\Omega_c^4}\left(1 - \frac{8f\omega}{\Omega_c}\right). \tag{60}$$

Here S and T are two new parameters which are much smaller than Q, because they depend on higher orders of x. In this case, it can also be proven that there are no solitons, and the only valid solution remains to be the wave train.

VI. CONCLUSIONS

We studied the nonlinear evolution of an Alfvén wave propagating along an ambient magnetic field in a strongly magnetized electron-positron plasma with relativistic temperatures. We derived a nonlinear Schrödinger equation for this circularly polarized electromagnetic wave in the normal dispersion zone. In this case the necessary condition for a modulational instability is fulfilled. We calculated the maximum growth rate for the instability and this growth rate decreases as the temperature increases, consistent with previous results [39,40]. This modulational instability admits an envelope soliton solution. As in the weakly magnetized case [40], with the increase of the temperature the envelope soliton becomes wider. We have also studied the Alfvén wave propagation in the anomalous dispersion zone, where there is no soliton solution and the only physical solution is a periodic wave train.

These results may have relevance in the study of the propagation of electromagnetic waves in environments where electron-positron plasmas are important, such as the propagation of the radio emissions through the pulsar's magnetosphere [17], the bulk acceleration of relativistic jets [18], or the emissions in quasar relativistic jets [19], among others.

ACKNOWLEDGMENTS

We thank CONICyT for support through FONDECyT Grants No. 1110135 (J.A.V.), No. 1110729 (J.A.V.), No. 1080658, and No. 1121144 (V.M.). R.A.L. thanks CONICyT for support through a Doctoral Fellowship, Contract No. 21100839. F.A.A. thanks CONICyT for support through a Becas Chile Postdoctoral Fellowship No. 74110049. A.C.L.C. thanks the CNPq for support, the European Commission for a Marie Curie International Incoming Fellowship, and the Paris Observatory for hospitality.

[1] G. Björnsson, M. A. Abramowicz, X. Chen, and J.-P. Lasota, Astrophys. J. **467**, 99 (1996).

[2] E. P. T. Liang, Astrophys. J. **234**, 1105 (1979).

[3] T. R. White and A. P. Lightman, Astrophys. J. **340**, 1024 (1989).

[4] G. W. Gibbons, S. Hawking, and S. T. C. Siklos (eds.), *The Very Early Universe* (Cambridge University Press, Cambridge, 1985).

[5] T. Tajima and T. Taniuti, Phys. Rev. A **42**, 3587 (1990).

[6] M. F. Curtis, *The Theory of Neutron Stars Magnetospheres* (University of Chicago Press, Chicago, 1991).

[7] Y. N. Istomin and D. N. Sobyanin, Astron. Lett. **33**, 660 (2007).

[8] V. V. Usov, Phys. Rev. Lett. **80**, 230 (1998).

[9] D. B. Blaschke, A. V. Prozorkevich, C. D. Roberts, S. M. Schmidt, and S. A. Smolyansky, Phys. Rev. Lett. **96**, 140402 (2006).

[10] G. P. Zank and R. G. Greaves, Phys. Rev. E **51**, 6079 (1995).

[11] P. Helander and D. J. Ward, Phys. Rev. Lett. **90**, 135004 (2003).

[12] P. Goldreich and W. H. Julian, Astrophys. J. **157**, 869 (1969).

[13] A. N. Timokhin and J. Arons, Mon. Not. R. Astron. Soc. **429**, 20 (2013).

[14] A. K. Harding, Astrophys. J. **300**, 167 (1986).

[15] A. A. da Costa, D. A. Diver, and G. A. Stewart, Astron. Astrophys. **366**, 129 (2001).

[16] S. Matsukiyo and T. Hada, Astrophys. J. **692**, 1004 (2009).

[17] Q. Luo, D. B. Melrose, and D. Fussell, Phys. Rev. E **66**, 026405 (2002).

[18] S. Iwamoto and F. Takahara, Astrophys. J. **565**, 163 (2002).

[19] J. F. C. Wardle, D. C. Homan, R. Ojha, and D. H. Roberts, Nature **395**, 457 (1998).

[20] J. T. Gosling, R. M. Skoug, D. J. McComas, and C. W. Smith, J. Geophys. Res. **110**, A01107 (2005).

[21] T. D. Phan *et al.*, Nature **439**, 175 (2006).

[22] A. C.-L. Chian and P. R. Muñoz, Astrophys. J. Lett. **733**, L34 (2011).

[23] C. H. Jaroschek, R. A. Treumann, H. Lesch, and M. Scholer, Phys. Plasmas **11**, 1151 (2004).

[24] M. Swisdak, Y.-H. Liu, and J. F. Drake, Astrophys. J. **680**, 999 (2008).

[25] S. Zenitani and M. Hoshino, Astrophys. J. **677**, 530 (2008).

[26] N. Bessho and A. Bhattacharjee, Astrophys. J. **750**, 129 (2012).

[27] B. Cerutti, G. R. Werner, D. A. Uzdensky, and M. C. Begelman, Astrophys. J. Lett. **754**, L33 (2012).

[28] J. Arons, Int. J. Mod. Phys. D **17**, 1419 (2008).

[29] M. Kino, N. Kawakatu, and F. Takahara, Astrophys. J. **751**, 101 (2012).

[30] G. Weidenspointner *et al.*, Nature **451**, 159 (2008).

[31] T. S. Pedersen, J. R. Danielson, C. Hugenschmidt, G. Marx, X. Sarasola, F. Schauer, L. Schweikhard, C. M. Surko, and E. Winkler, New J. Phys. **14**, 035010 (2012).

[32] A. C.-L. Chian and C. F. Kennel, Astrophys. Space Sci. **97**, 9 (1983).

[33] E. Asseo and A. Riazuelo, Mon. Not. R. Astron. Soc. **318**, 983 (2000).

[34] M. Y. Yu, P. K. Shukla, and L. Stenflo, Astrophys. J. **309**, L63 (1986).

[35] F. B. Rizatto, R. S. Schneider, and D. Dillenburg, Phys. Lett. A **133**, 59 (1988).

[36] T. Cattaert, I. Kourakis, and P. K. Shukla, Phys. Plasmas **12**, 012319 (2005).

[37] S. M. Mahajan, Phys. Rev. Lett. **90**, 035001 (2003).

[38] F. A. Asenjo, V. Muñoz, J. A. Valdivia, and T. Hada, Phys. Plasmas **16**, 122108 (2009).

[39] R. López, F. A. Asenjo, V. Muñoz, and J. A. Valdivia, Phys. Plasmas **19**, 082104 (2012).

[40] F. A. Asenjo, F. A. Borotto, Abraham C.-L. Chian, V. Muñoz, J. A. Valdivia, and E. L. Rempel, Phys. Rev. E **85**, 046406 (2012).

[41] V. I. Berezhiani and S. M. Mahajan, Phys. Rev. E **52**, 1968 (1995).

[42] A. Hasegawa, *Plasma Instabilities and Nonlinear Effects* (Springer-Verlag, Berlin, 1975).

[43] K. Nishikawa and C. S. Liu, in *Advances in Plasma Physics*, edited by A. Simon and W. B. Thompson (Wiley, New York, 1976), Vol. 6, Chap. 2, pp. 3–81.

[44] F. F. Chen, *Introduction to Plasma Physics and Controlled Fusion* (Plenum Press, New York, 1990).

[45] A. Ebaid and S. M. Khaled, J. Comput. Applied Math. **235**, 1984 (2011).